Chaos, Solitons and Fractals 103 (2017) 476–487

Contents lists available at ScienceDirect

Chaos, Solitons and Fractals

Nonlinear Science, and Nonequilibrium and Complex Phenomena

journal homepage: www.elsevier.com/locate/chaos

Chaotic chameleon: Dynamic analyses, circuit implementation, FPGA design and fractional-order form with basic analyses

Karthikeyan Rajagopal[a], Akif Akgul[b,*], Sajad Jafari[c], Anitha Karthikeyan[d], Ismail Koyuncu[d]

[a] Centre for Non-Linear Dynamics, Defense University, Ethiopia
[b] Department of Electrical and Electronics Engineering Faculty of Technology, Sakarya University, Sakarya, Turkey
[c] Biomedical Engineering Department, Amirkabir University of Technology, Tehran, Iran
[d] Department of Electrical and Electronics Engineering, Faculty of Technology, Afyon Kocatepe University, Afyon, Turkey

ARTICLE INFO

Article history:
Received 27 April 2017
Revised 11 June 2017
Accepted 7 July 2017

Keywords:
Hidden attractors
Self-excited attractors
Electronic circuit implementation
Chaotic oscillators
FPGA
Fractional-order chaotic systems
Dynamical analyses

ABSTRACT

There are many recent investigations on chaotic systems with self-excited and hidden attractors. In this paper we introduce a chaotic system in which the attractor can change between hidden and self-excited attractor depending on the value of parameters. Dynamical properties of the proposed attractor are investigated. The attractor is then realized using off the shelf components. Also, for this new system electronic circuit is implemented and FPGA-based chaotic oscillator is designed. In the end, the fractional- order form is examined through bifurcation and stability analysis.

© 2017 Elsevier Ltd. All rights reserved.

1. Introduction

Dynamical systems can be categorized into systems with self-excited attractors and systems with hidden attractors [1–3].A self-excited attractor has a basin of attraction that is associated with an unstable equilibrium, while a hidden attractor has a basin of attraction that does not intersect with small neighborhoods of any equilibrium points. Hidden attractors are important in many engineering problems as they allow unexpected responses [4,5]. Control of such hidden oscillations is a big challenge because of their multi-stable nature [6,7]. Chaotic attractors with no equilibrium points [8–11,11–15], with only stable equilibria [16,17] and with curves of equilibria [18] are widely discussed in literatures recently. Fractional order no equilibrium systems with its FPGA implementation have also been reported recently [19,20]. A no equilibrium fractional order hyperchaotic system is proposed and investigated in [21].

The first chaotic circuit was designed by Chua [22]. This circuit has been used in applications like chaos-based generator. Later, some more different chaotic electronic circuits such as simple RLC, RC circuits [23–25], oscillators [26,27] and capacitor circuits were introduced. Many different chaotic and hyper chaotic systems have been realized in literature which in order to prove that the solutions are not numerical errors [28–41].

FPGA chips are programmable integrated circuit devices for digital circuit designs. FPGA chips allow designers to make designs wherever they want, even after chip manufacturing has been completed [42]. FPGA chips have very high capacity and speed. These chips are often called System on a Chip (SoC). In addition, they can work as part of larger systems with other chips, when needed [43]. Today, there are FPGA chips with an operational frequency of approximately 1 GHz. Although FPGA chips have lower operational frequency compared to personal computers, they can perform operations much faster than the personal computers thanks to its advantages such as parallel operation and system specific design. Another advantage of FPGA chips is that they can run more than one copy of a designed system inside the chip and achieve very high speed advantages. In addition, FPGA chips are used as prototypes for ASIC-based applications because of their low cost and reprogramming capabilities. [44]. Today FPGA chips are widely used in many fields such as image processing [45], pseudo and true random number generator [46–48], communication [49], pseudo and true, control [50], and artificial neural networks [51,52].

* Corresponding author.
E-mail addresses: rkarthiekeyan@gmail.com (K. Rajagopal), aakgul@sakarya.edu.tr (A. Akgul), sajadjafari83@gmail.com (S. Jafari), mrs.anithakarthikeyan@gmail.com (A. Karthikeyan), ismailkoyuncu@aku.edu.tr (I. Koyuncu).

http://dx.doi.org/10.1016/j.chaos.2017.07.007
0960-0779/© 2017 Elsevier Ltd. All rights reserved.

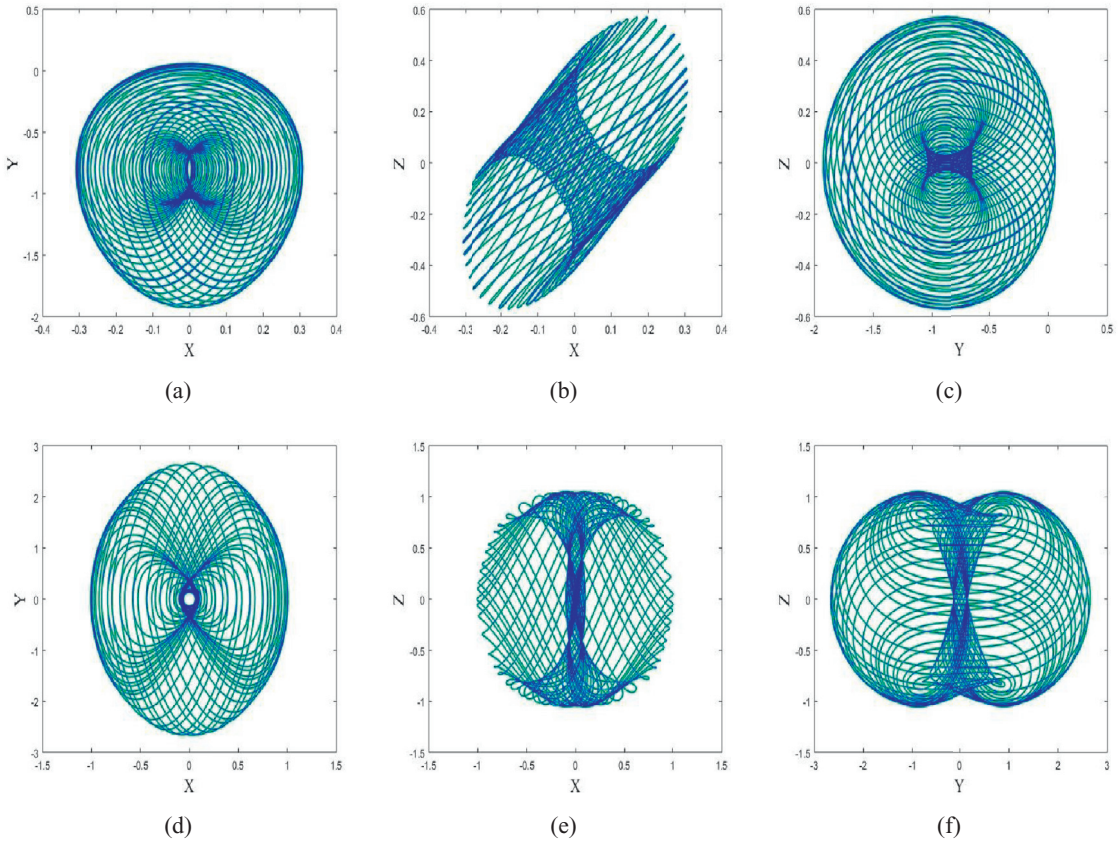

Fig. 1. 2D phase portraits of the self-excited attractor with $b = 0.8$: (a) x, y; (b) x, z; (c) y, z. 2D phase portrait of the hidden attractor with $b = 0$: (d) x, y; (e) x, z; (f) y, z.

A fractional-order chaotic system is asymmetric, dissimilar, and topologically inequivalent to typical chaotic systems. It challenges the conventional notion that the presence of unstable equilibria is mandatory to ensure the existence of chaos [53,54]. A fractional order chaotic system without equilibrium point is discussed in [55]. Fractional calculus and its application in engineering and science have drawn attention in the last decade [56–59]. Various control approaches with fractional order are also discussed in [60–62]. A novel fractional order no equilibrium chaotic system is investigated in [54] and a fractional order hyper-chaotic system without equilibrium points is investigated in [55]. Memristor based fractional order system with a capacitor and an inductor is discussed [63]. Numerical analysis and methods for simulating fractional order nonlinear system is proposed in [64] and Matlab solutions for fractional order chaotic systems is discussed in [65]. Current through the capacitor and voltage in the inductor are applicable for an ideal condition. If the losses of the capacitor and proximity effect of the inductor is included then the derivative in their equations actually become fractional order derivative [66].

Recently a 3D chaotic system which can have three famous categories of hidden attractors plus systems with self-excited attractors was discussed in [67]. A hyper-chaotic system which behaves like a chameleon with both self-excited and hidden flows was discussed in [68]. Motivated by this, in this paper we announce a chaotic system which can have self-excited or hidden attractor depending on the values of the parameters. This system helps us to better understand the hidden chaotic flows which can change in parameter space.

In Section 2, chaotic chameleon system is introduced and its dynamical properties are analyzed. In Sections 3 and 4, circuit realization and FPGA design will be carried out. In Section 5, fractional-order form and its dynamic analyses of the proposed system are presented through bifurcation and stability analysis. The last section provides conclusions and future works.

2. Chaotic chameleon system and its dynamic properties

In this section we propose a novel chaotic system which we have named as chaotic chameleon for the reason that the system shows self-excited and hidden oscillations depending on the value of parameter. Table 1 shows the chaotic system and its parameter values.

The initial conditions of the system are taken as [0.1, 0.01,0.01]. Fig. 1 shows the 2D phase portraits of the self-excited and hidden attractors.

2.1. Equilibrium points

The equilibrium points of 3D chaotic amphibian system depends on the parameter b and is given by the $x = \pm 3.5\sqrt{12.25(a-b^2)}; y = -b; z = \mp\frac{1}{2b}\sqrt{12.25(a-b^2)}$. The system has no equilibrium when $b = 0$. It has an unstable equilibrium $E_{1,2} = \pm 0.4, -0.8, \mp 0.8750$ when $b = 0.8$. The Eigen values of the system at E_1 are $\lambda_{1,2} = -1.8497 \pm 3.0720i, \lambda_3 = 0.2034$ where λ_3 is the unstable node and the eigen values of the system at E_2 are $\lambda_{1,2} = 1.8497 \pm 3.0720i, \lambda_3 = -0.2034$ where $\lambda_{1,2}$ is the unstable spiral point and thus SA system is a self-excited attractor for both the equilibriums. The characteristic equations for the system at $E_{1,2}$ are $\lambda^3 \pm 3.49\lambda^2 + 12.10\lambda \mp 2.62$. As per Routh-Hurwitz criterion, all the principal minors need to be positive for the

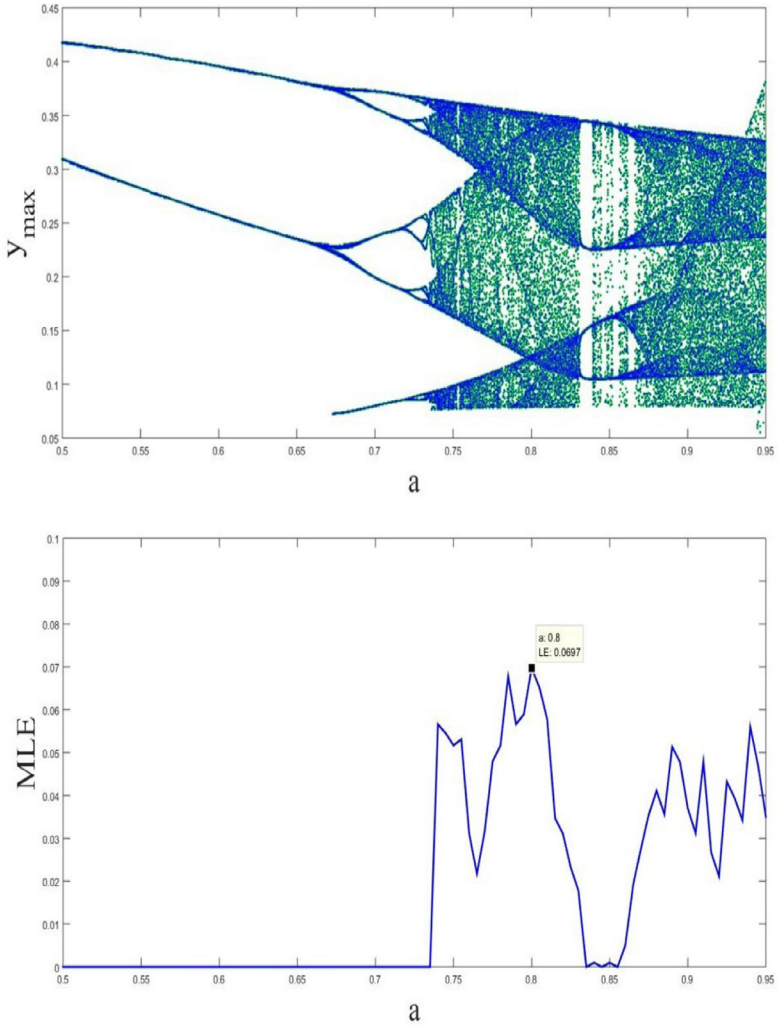

Fig. 2. Bifurcation plot and corresponding maximum Lyapunov exponent (MLE) of the chaotic chameleon system for parameter a with parameter $b = 0.8, c = 0.01$ and initial conditions [0.1, 0.01, 0.01].

Table 1
Chaotic chameleon.

Chaotic system	System name	Parameters	Type of system
$\dot{x} = y + b$	SA		Self-excited attractor (b=0.8)
$\dot{y} = -7x + 4yz$		$a = 0.8;\ c = 0.01$	
$\dot{z} = a - x^2 - y^2 + cxz$	HA		Hidden attractor (b=0)

proposed system to be stable. The principal minors are,

$$\Delta_1 = \delta_1 > 0, \Delta_2 = \begin{vmatrix} \delta_1 & \delta_0 \\ \delta_3 & \delta_2 \end{vmatrix} > 0, \Delta_3 => \begin{vmatrix} \delta_1 & \delta_0 & 0 \\ \delta_3 & \delta_2 & \delta_1 \\ 0 & 0 & \delta_3 \end{vmatrix} > 0 \tag{1}$$

where $\delta_0 = 1, \delta_1 = 3.5 - 0.1c, \delta_2 = 12.12 - 1.4c, \delta_3 = -5.6c - 2.56$ for equilibrium E_1 and for E_2 the values are $\delta_0 = 1, \delta_1 = -3.5 + 0.1c, \delta_2 = 12.12 - 1.4c, \delta_3 = 5.6c + 2.56$. For the parameter values of $a = 0.8, b = 0.8, c = 0.01$ it is clear that $\Delta_2 < 0$ and hence the equilibrium is unstable.

2.2. Lyapunov exponents and Kaplan-Yorke dimension

In a dynamical system, the existence of a positive Lyapunov exponents confirms the chaotic behavior of the system [69–73]. Calculating accurate Lyapunov Exponents (LEs) is necessary to detect chaos and hyper chaos in dynamical systems. A definition of LEs for fractional differential systems was given in [69] based on frequency-domain approximations, but the limitations of frequency-domain approximations are highlighted in [73]. Time series based LEs calculation methods like Wolf algorithm [70], Jacobian method [71] and neural network algorithm [72] are popularly known ways of calculating Lyapunov exponents for integer and fractional order systems. In this paper we use the Jacobian

Table 2
Lyapunov exponents and KY dimension of chaotic chameleon systems.

Attractor	Lyapunov exponents	KY dimension
Self-excited	L_1=0.0697, L_2= 0, $L_3 = -0.0838$	2.832
Hidden	L_1=0.0526, L_2= 0, $L_3 = -0.0711$	2.739

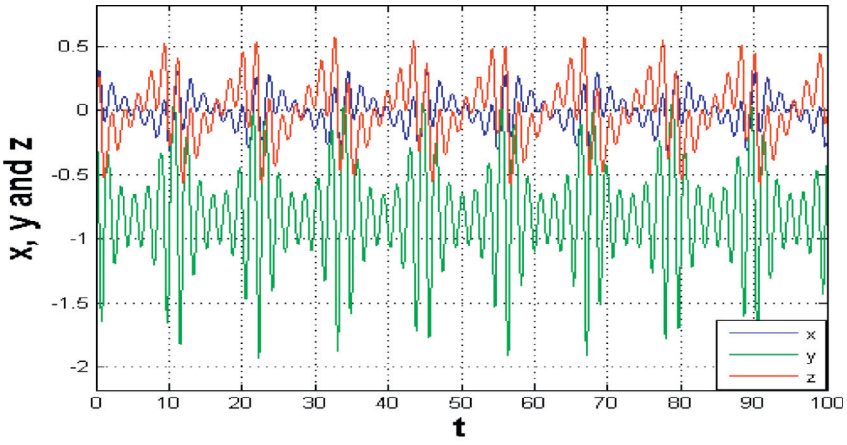

(a)

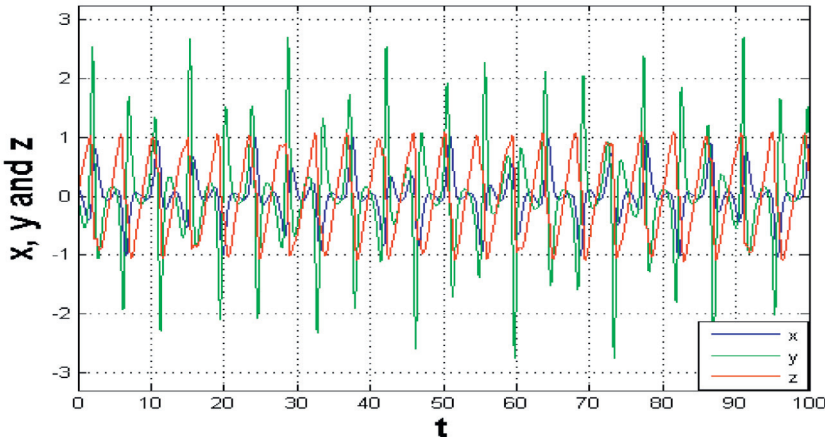

(b)

Fig. 3. (a) The time series signals of self-excited attractor for x, y and z outputs. (b) The time series signals of hidden attractor for x, y and z outputs.

method to calculate the LEs. Table 2 shows the Lyapunov exponents of the NCS chaotic systems.

2.3. Bifurcation

To study the parameter dependence of the proposed chaotic chameleon, we investigate the bifurcation of the system in parameter space. The parameter a is considered as the bifurcation parameter while the parameter b and c are fixed at its value. The initial conditions for the first iteration are [0.1, 0.01, 0.01] and its reinitialized to the end values of the state trajectories after every iteration. The initial transients are discarded and the peaks of each states for every iteration is plotted. As can be seen in Fig. 2, the bifurcation plot of chaotic chameleon system shows that the system enters in to chaotic region with routine period doubling. Also, the corresponding maximum Lyapunov exponent (MLE) of the chaotic chameleon system for parameter a with parameter $b = 0.8, c = 0.01$ and initial conditions [0.1, 0.01, 0.01] are seen in Fig. 2.The first chaotic region is seen for $0.74 \leq a \leq 0.84$. The systemâs largest Lyapunov exponent is seen when $a = 0.8$. The system shows limit cycles for $0.84 \leq a \leq 0.88$. The system enters in to the second chaotic regime for $0.88 \leq a \leq 0.95$.

3. Circuit implementations of the chaotic chameleon system

In this section, the electronic circuit applications of self-excited and hidden chaotic chameleon systems (Table 1) have been executed on the oscilloscope. The chameleon system is self-excited attractor as parameter $b = 0.8$ and hidden attractor as parameter $b = 0$. The two electronic circuit applications are implemented for different chaotic behaviors.

Fig. 3(a) and (b) show the time series signals of the self-excited and hidden attractors respectively. Signal values are between 3 V and −3 V as seen as figures. The signal values don't need to be scaled for real-time application because of amplitude values are in the linear range of operator amplifiers for electronic design. So, the electronic circuit application can directly be done without scale process. A electronic circuit is designed as shown in Fig. 4. While the switch is in position 2, electronic circuit is for self-excited attractor. In other position (while switch 1), it is hidden attractor.

R1 = 400 KΩ, R2 = R5 = 7485 KΩ, R3 = 57 KΩ, R4 = 10 KΩ, R6 = 4000 KΩ, R7 = R8 = 40 KΩ, R9 = R10 = 100 KΩ, C1 = C2 = C3 = 1 nF, Vn = -15 V, Vp = 15 V were chosen. Fig. 5(a)–(c) and Fig. 5(d)–(f) show the oscilloscope outputs which is experimental phase portraits of the self-excited and hidden attractors respectively. The oscilloscope outputs and Matlab simulation results are similar as seen as Figs. 1,2 and 5.

4. FPGA-based chaotic chameleon oscillator

In this section, new continuous-time chaotic chameleon oscillator presented has been designed and implemented on a discrete-time basis on FPGA. Chaotic chameleon oscillator has been designed using VHDL (Very High Speed Integrated Circuit Hardware

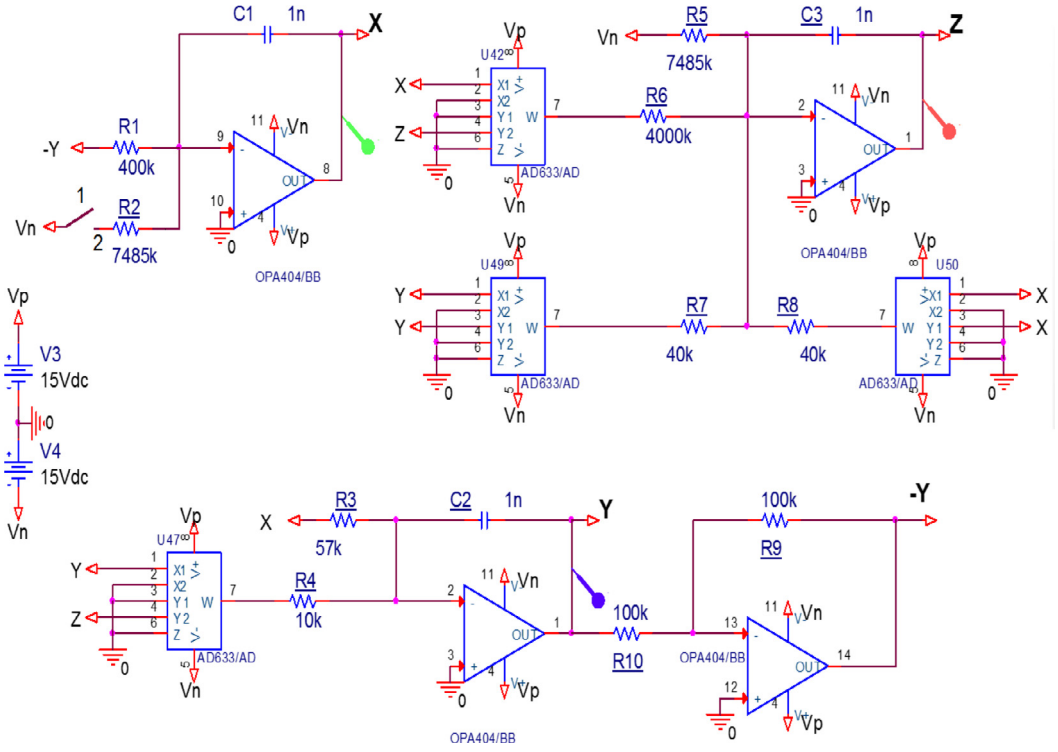

Fig. 4. The electronic circuit schematic of the chameleon chaotic system.

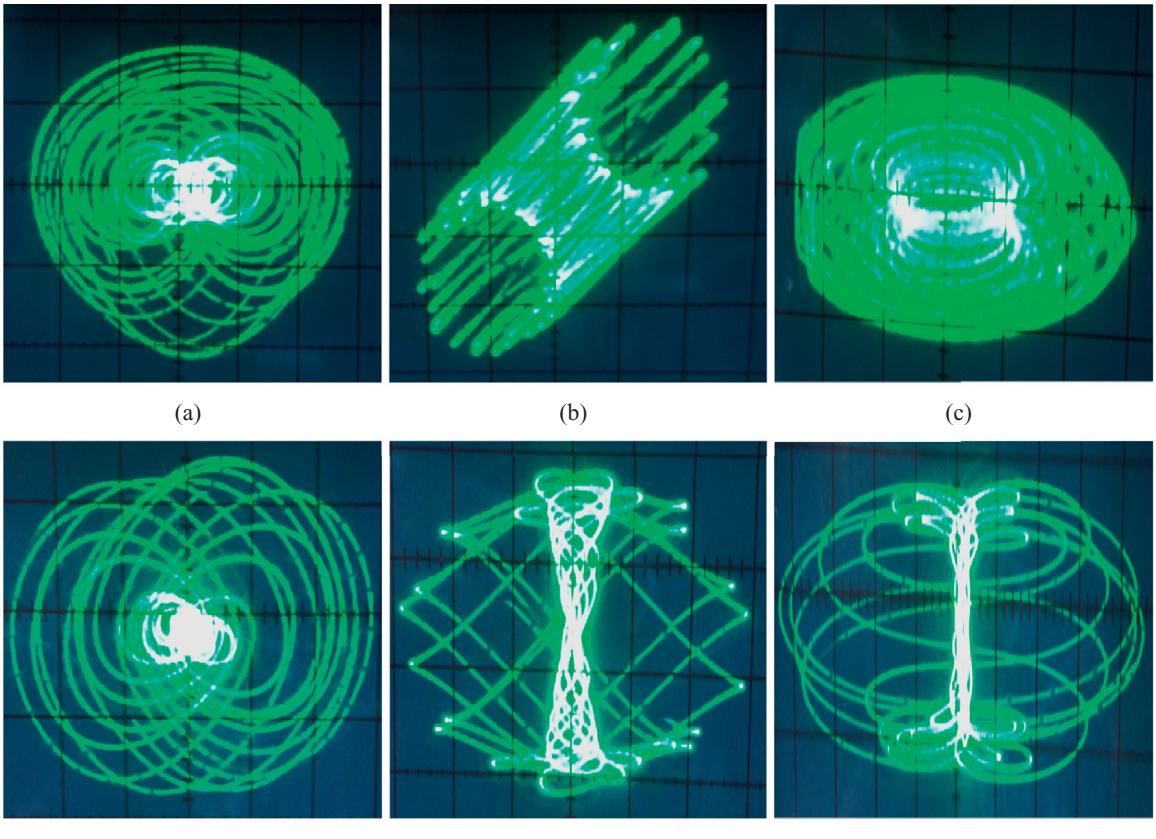

Fig. 5. The phase portraits of chameleon chaotic system for self-excited attractor: (a) *x, y*; (b) *x, z*; (c) *y, z*. The phase portraits of chameleon chaotic system for hidden attractor: (d) *x, y*; (e) *x, z*; (f) *y, z*.

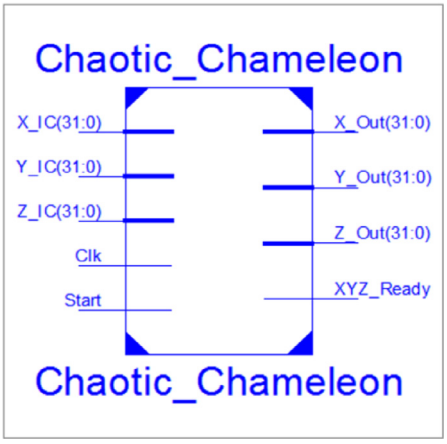

Fig. 6. Top level block diagram of the FPGA-based chaotic chameleon oscillator unit.

Description Language) and 32-bit IEEE-754-1985 floating point number standard. Design and test phases have been carried out with Xilinx ISE Design Tools 13.4 (X-ISE-DT). In order to model the continuous-time chaotic chameleon oscillator on the FPGA as discrete time, the fifth order Runge-Kutta Butcher (RK5B) algorithm having high precision has been used. RK5B algorithm is given in Eq. (2). RK5B algorithm consists of six steps that are k1, k2, k3 and k4, k5 and k6. Structurally, RK5B algorithm generates more precise results than the Euler, Heun and RK4 algorithms. Here, Δh is the number of algorithm step y_λ is the first initial value that the system requires for the algorithm, and $y_{\lambda+1}$ is the next calculated discrete time value of the system. In this study, FPGA-based chaotic chameleon oscillator is taken as $\Delta h = 0.05$.

$$y_{\lambda+1} = y_\lambda + \frac{1}{90}(7k_1 + 32k_3 + 12k_4 + 32k_5 + 7k_6)\Delta h$$
$$k_1 = f(y_\lambda)$$
$$k_2 = f(y_\lambda + \frac{\Delta h}{4}k_1)$$
$$k_3 = f(y_\lambda + \frac{\Delta h}{8}k_1 + \frac{\Delta h}{8}k_2)$$
$$k_4 = f(y_\lambda - \frac{\Delta h}{2}k_2 + \Delta h k_3)$$
$$k_5 = f(y_\lambda + \frac{3\Delta h}{16}k_1 + \frac{9\Delta h}{16}k_4)$$
$$k_6 = f(y_\lambda - \frac{3\Delta h}{7}k_1 + \frac{2\Delta h}{7}k_2 + \frac{12\Delta h}{7}k_3 - \frac{12\Delta h}{7}k_4 + \frac{8\Delta h}{7}k_5) \quad (2)$$

X-ISE-DT program top level block diagram obtained by modeling FPGA-based chaotic chameleon oscillator in VHDL with RK5B algorithm is given in Fig. 6. The 1-bit Start and Clk signals at system inputs are used to enable synchronization of the sub-modules in the oscillator. x_0, y_0 and z_0 initial conditions required by the system at the time of initial operation are enabled by 32-bit X-IC, Y-IC and Z-IC input signals. 32-bit X-Out, Y-Out and Z-Out signals refer to the oscillator output. When output is generated from X-Out, Y-Out and Z-Out signals, XYZ-Ready signal is '1'and it is '0' in other cases.

The second level block diagram of the FPGA-based chaotic chameleon oscillator unit is given in Fig. 7. Chaotic chameleon oscillator is divided into two parts as Mux (Multiplexer) and Chameleon-RK5B units. Mux unit is designed to provide the initial conditions that the system requires during the initial operation and subsequent operations. Ready signal is '0' until the Chameleon-RK5B unit generates result and the system receives the starting conditions externally. When the Ready signal is '1', Mux unit receives the signals from the Chameleon-RK5B unit and sends it to the input as starting condition to enable the oscillator to generate the next value.

The third level block diagram of the FPGA-based chaotic chameleon oscillator unit is given in Fig. 8. Six unit k_1, k_2, k_3 and k_4, k_5 and k_6 in the unit are designed to calculate RK5B algorithm parameters. ys unit calculates the next $y_{\lambda+1}$ values of the oscillator and sends these values to the filter unit. Filter unit is designed to filter out the signals when there are undesired signals. The designed FPGA-based chaotic chameleon oscillator generates the first output signal at the end of 307 clock cycle and at the end of each 307 clock cycle, it sends the new X-Out, Y-Out and Z-Out signals to the output.

In this study, two different FPGA-based chaotic chameleon oscillators have been designed for $b = 0.8$ (self-excited attractor) and $b = 0$ (hidden attractor).Figs. 9 and 10 show the simulation results obtained from the X-ISE-DT simulator for two different FPGA-based chaotic chameleon oscillators for $b = 0.8$ and $b = 0$. Although 32-bit IEEE-754-1985 floating point number standard has been used

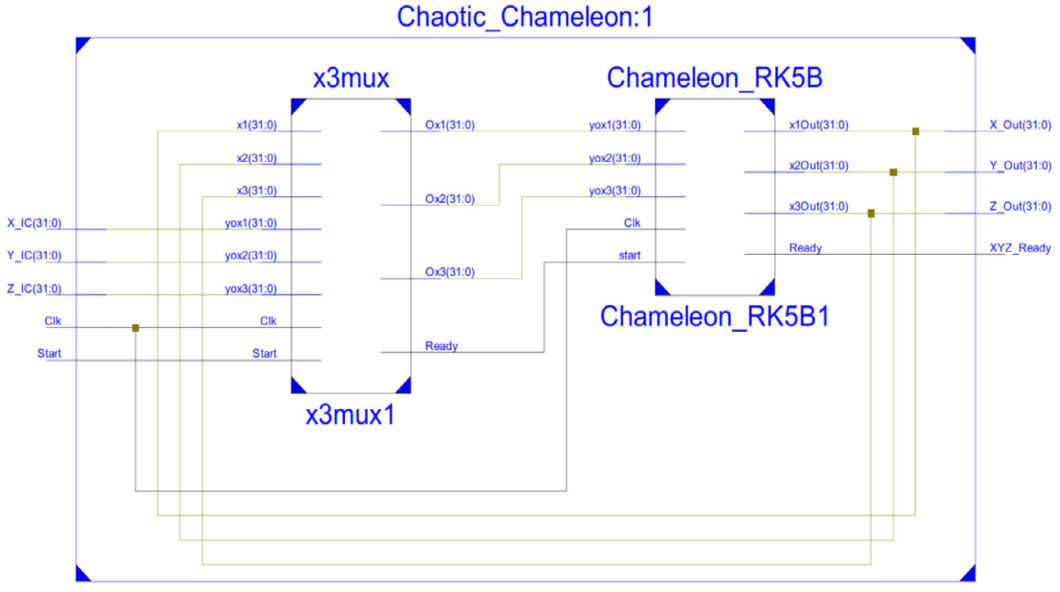

Fig. 7. Second level block diagram of the FPGA-based chaotic chameleon oscillator unit.

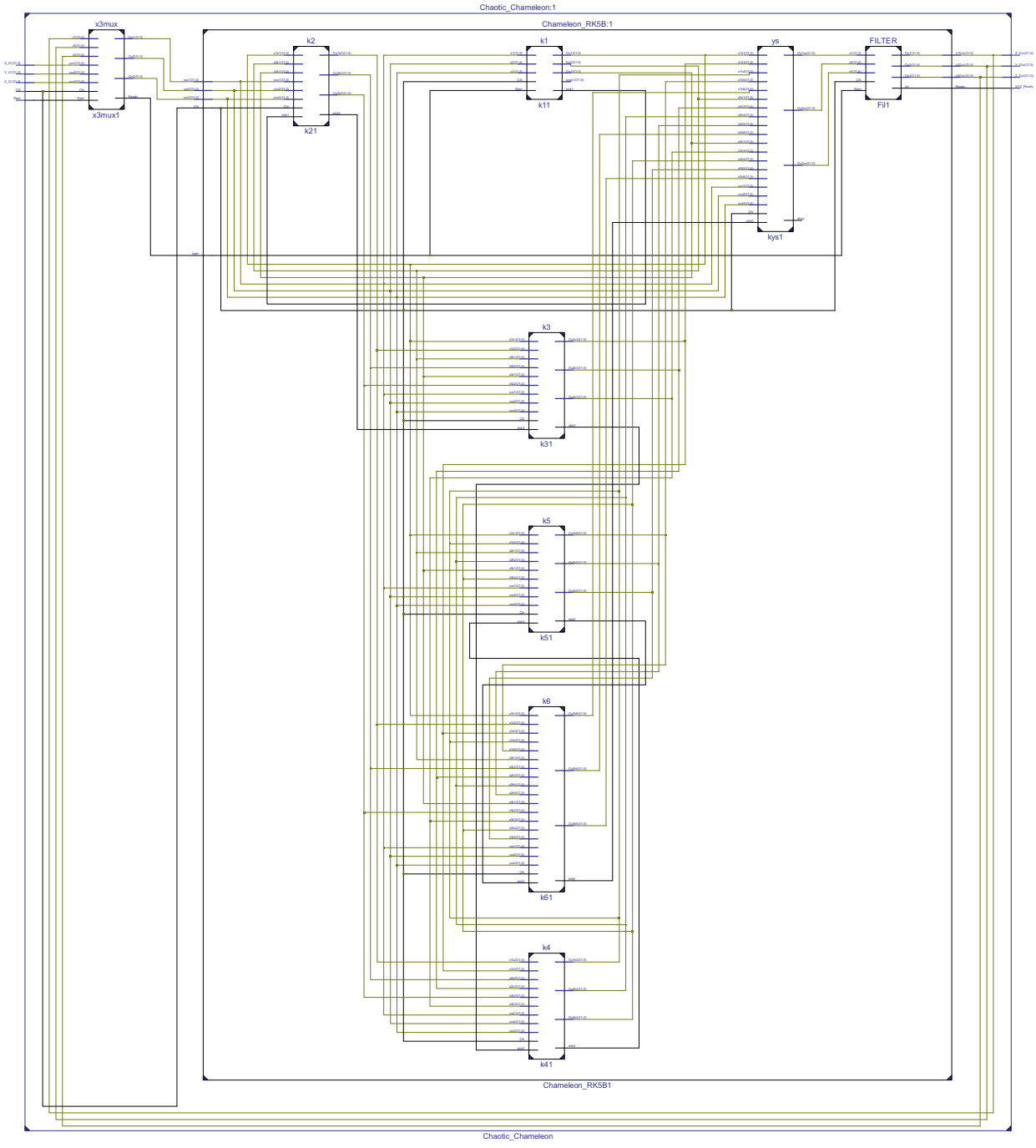

Fig. 8. Third level block diagram of the FPGA-based chaotic chameleon oscillator unit.

in design of FPGA-based chaotic chameleon oscillator, it has been shown in hexadecimal format in the simulator as it provides readability.

In addition, binary values in the 32-bit IEEE754-1985 format of the time series of X-Out, Y-Out and Z-Out signals obtained from the verification of the chaotic chameleon oscillator in the FPGA have been recorded in a file during the test phase. Recorded values have been converted to real number system. Then, the phase portraits have been plotted in the Matlab program by using the first 3x2400 data set (X-Out, Y-Out and Z-Out) generated by the FPGA-based chaotic chameleon oscillator. Phase portraits obtained from the verification of the chaotic chameleon oscillator on the FPGA are given in Fig. 11(a)–(c) for $b = 0.8$ and in Fig. 11(d)–(f) for $b = 0$.

Table 3 shows the Xilinx VIRTEX6 family XC6VLX240T-1FF1156 FPGA chip statistics obtained from place and route processing for FPGA-based chaotic chameleon oscillator $b = 0.8$ and $b = 0$. The minimum pulse period for self-excited attractor ($b = 0.8$) and hidden ($b = 0$) attractor units has been found as 3.070 ns.

5. Fractional order chaotic chameleon (FOCA) system and its dynamic analysis

In this section, we derive the fractional order model of the chaotic chameleon. There are three commonly used denition of the fractional-order dierential operator, viz. Grunwald-Letnikov, RiemannLiouville and Caputo [56–58]. We use the Grunwald-Letnikov

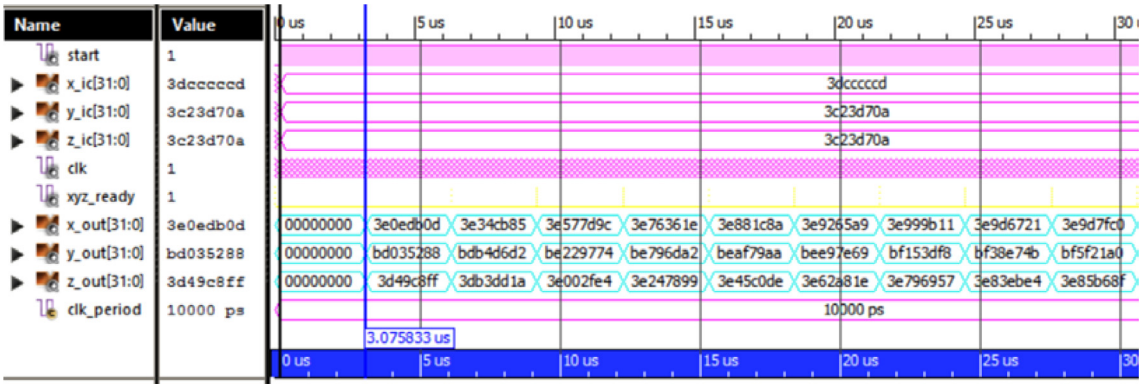

Fig. 9. X-ISE-DT simulator results for FPGA-based chaotic chameleon oscillator $b = 0.8$.

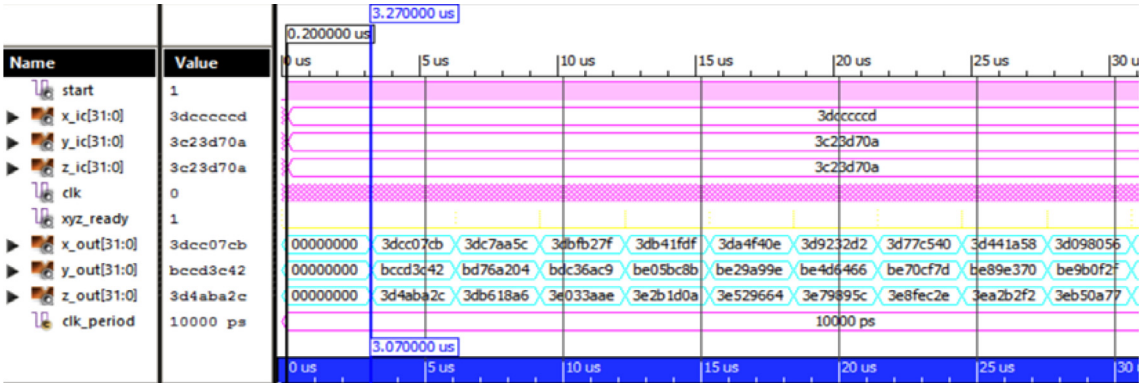

Fig. 10. X-ISE-DT simulator results for FPGA-based chaotic chameleon oscillator $b = 0$.

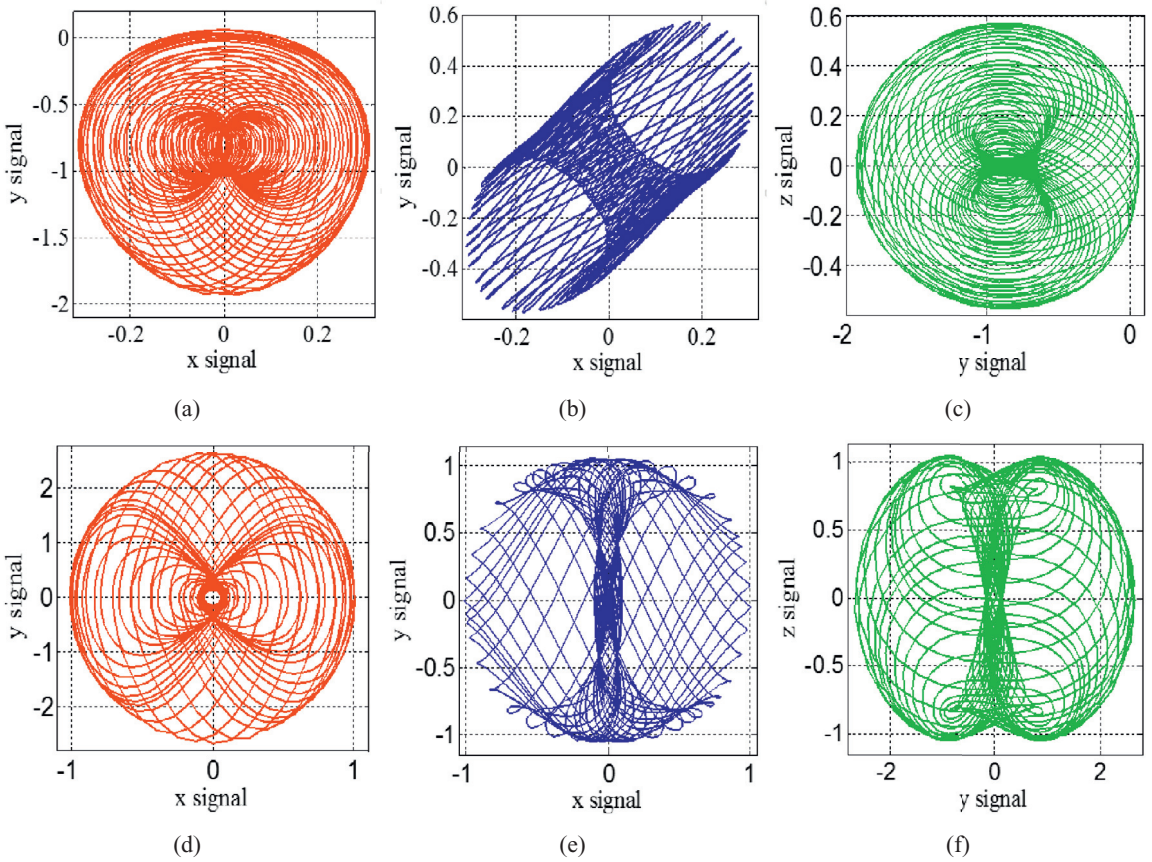

Fig. 11. 2D phase portraits of the FPGA-based self-excited attractor for $b = 0.8$: (a) x, y; (b) x, z; (c) y, z. 2D phase portraits of the FPGA-based self-excited attractor for $b = 0$: (d) x, y; (e) x, z; (f) y, z.

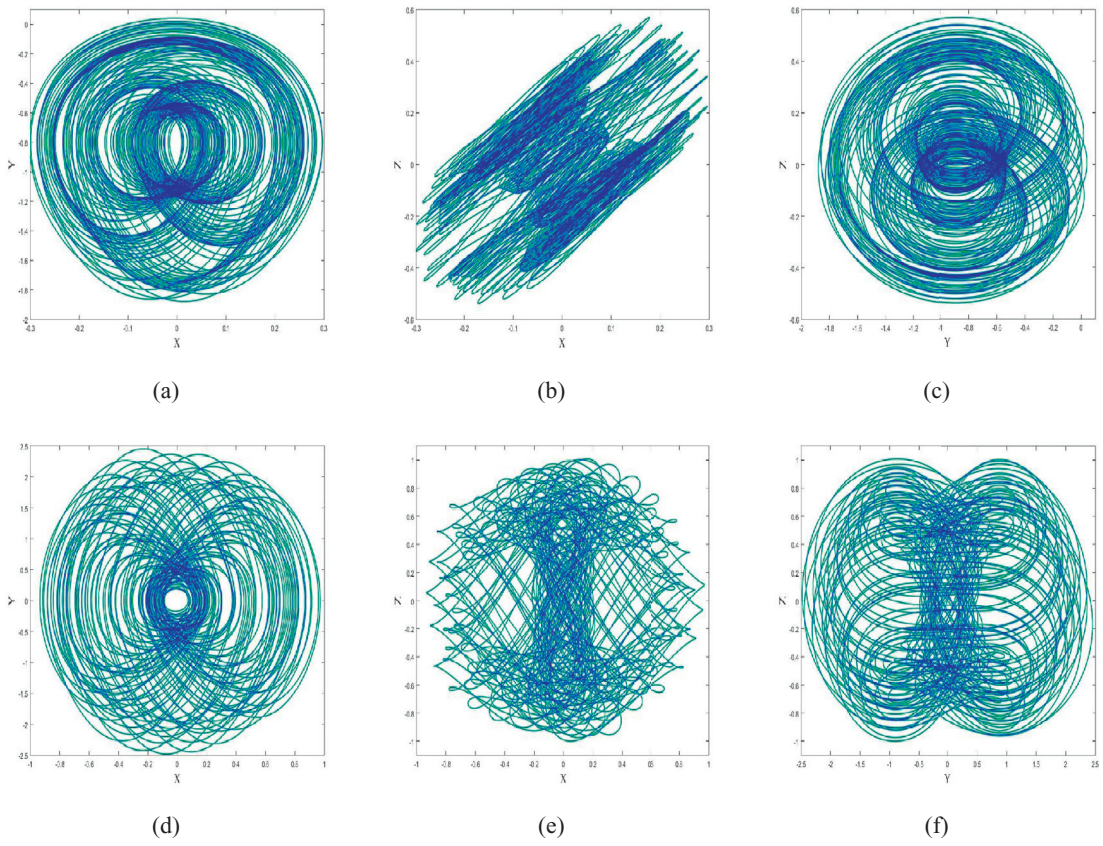

Fig. 12. 2D phase portraits of the self-excited fractional order chaotic chameleon with the commensurate fractional order of with $q = 0.997$: (a) x, y; (b) x, z; (c) y, z. 2D phase portraits of the hidden attractor fractional order chaotic chameleon with the commensurate fractional order with $q = 0.998$: (d) x, y; (e) x, z; (f) y, z.

Table 3
FPGA chip statistics of chaotic chameleon.

FPGA based chaotic chameleon	Number of Slice Regs. / %	Number of LUTs / %	Number of Bonded IOBs / %	Number of occupied Slices / %	Max. Clock Frequency (MHz)
b = 0.8	94323/31	89,129/59	195/32	27917/74	325.759
b = 0	92061/30	86,944/57	195/32	27901/72	325.759

(GL) definition, which is defined as

$$
\begin{aligned}
{}_aD_t^q f(t) &= \lim_{h\to 0}\left\{\frac{1}{h^q}\sum_{j=0}^{\left[\frac{t-a}{h}\right]}(-1)^j\binom{q}{j}f(t-jh)\right\}\\
&= \lim_{h\to 0}\left\{\frac{1}{h^q}\Delta_h^q f(t)\right\} \qquad (3)
\end{aligned}
$$

where a and t are limits of the fractional order equation, $\Delta_h^q f(t)$ is generalized difference, is the step size and q is the fractional order of the differential equation.

For numerical calculations the above equation is modified as

$$
{}_{(t-L)}D_t^q f(t) = \lim_{h\to 0}\left\{h^{-q}\sum_{j=0}^{N(t)} b_j(f(t-jh)\right\} \qquad (4)
$$

Theoretically fractional order differential equations use infinite memory. Hence when we want to numerically calculate or simulate the fractional order equations we have to use finite memory principal, where L is the memory length and h is the time sampling.

$$
N(t) = \min\left\{\left[\frac{t}{h}\right], \left[\frac{L}{h}\right]\right\} \qquad (5)
$$

The binomial coefficients required for the numerical simulation is calculated as,

$$
b_j = \left(1 - \frac{a+q}{j}\right)b_{j-1} \qquad (6)
$$

Using Eqs. (3)–(6), the fractional order chaotic chameleon system is derived as,

$$
\begin{aligned}
\frac{d^{q_x}x}{dt^{q_x}} &= y + b\\
\frac{d^{q_y}y}{dt^{q_y}} &= -7x + 4yz\\
\frac{d^{q_z}z}{dt^{q_z}} &= a - x^2 - y^2 + cxz \qquad (7)
\end{aligned}
$$

where q_x, q_y, q_z are the fractional orders of the chaotic chameleon system. Fig. 12 shows the 2D phase portraits of the self-excited and hidden attractor systems with the parameter and initial conditions as discussed in Section 2.

5.1. Bifurcation with fractional order

Most of the dynamic properties of the chaotic chameleon system like the Lyapunov exponents and bifurcation with parameters

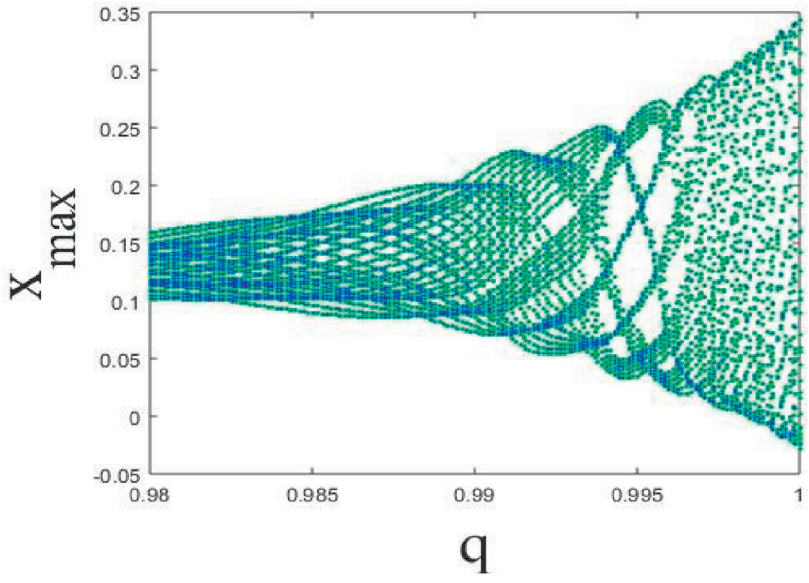

(a)

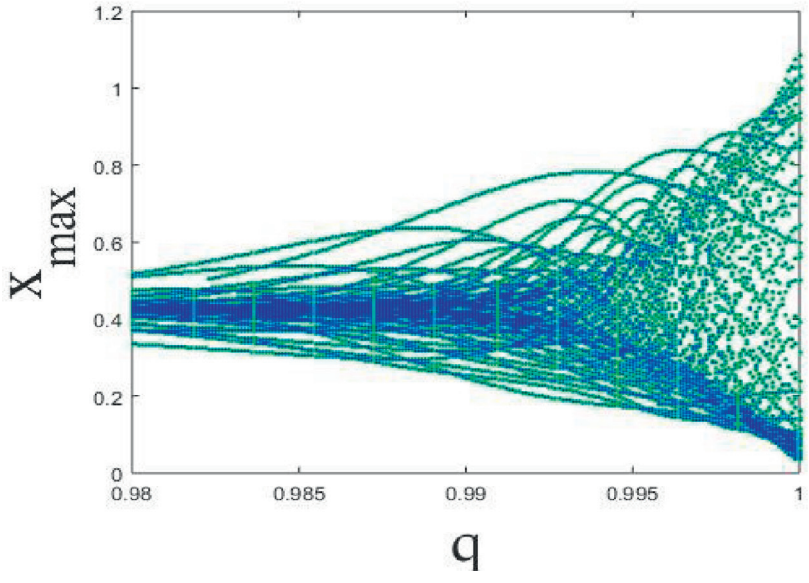

(b)

Fig. 13. (a) Bifurcation of fractional order chaotic chameleon (self-excited) system with order q (b) Bifurcation of fractional order chaotic chameleon (hidden) system with order q.

are preserved in the FOCA system [19,20] if $q_i > 0.995$ for self-excited and $q_i > 0.992$ hidden where $i = x, y, z$. The most important analysis of interest when investigating a fractional order system is the bifurcation with fractional order. As can be seen from figure 18 and 19 (self-excited and hidden), bifurcation of the fractional order chaotic chameleon system for change in fractional order shows that the systems chaotic oscillations remains if $q_i > 0.995$ for self-excited and $q_i > 0.992$ hidden where $i = x, y, z$ and the largest positive Lyapunov exponent ($L_1 = 0.0713$) of the self-excited system appears when $q > 0.997$ against its largest integer order Lyapunov exponent ($L_1 = 0.0697$) and similarly the largest positive Lyapunov exponent ($L_1 = 0.0553$) of the hidden attractor system appears when $q > 0.998$ against its largest integer order Lyapunov exponent ($L_1 = 0.0526$) (Fig. 13).

5.2. Stability analysis

Commensurate Order: For commensurate fractional order chaotic chameleon system of order q, the system is stable and exhibits chaotic oscillations if $|\arg(eig(J_E))| = |\arg(\lambda_i)| > \frac{q\pi}{2}$ where J_E is the Jacobian matrix at the equilibrium E and λ_i are the Eigen values of the system where $i = 1, 2, 3$. As seen from the system, the Eigen values should remain in the unstable region and the necessary condition for the fractional order chaotic chameleon system to be stable is $q > \frac{2}{\pi}\tan^{-1}\left(\frac{|\mathrm{Im}\lambda|}{\mathrm{Re}\lambda}\right)$. The chaotic system shows two equilibrium at E_1 and E_2 and the characteristic equation for the commensurate orders $q = 0.99$ for the equilibrium points $E_{1,2}$ is given by $\lambda^{297} + 3\lambda^{199} \pm 3.49\lambda^{198} + 3\lambda^{101} \pm 6.99\lambda^{100} + 12.1\lambda^{99} + \lambda^3 \pm 3.49\lambda^2 + 12.1\lambda \mp 2.616$.

Incommensurate Order: The necessary condition for the FOCA system to exhibit chaotic oscillations in the incommensurate case is, $\frac{\pi}{2M} - \min_i(|\arg(\lambda i)|) > 0$ where M the LCM of the fractional orders. If $q_x = 0.97, q_y = 0.98, q_z = 0.99$, then $M = 100$. The characteristic equation of the system evaluated at the equilibriums are $\det(diag[\lambda^{Mq_x}, \lambda^{Mq_y}, \lambda^{Mq_z}] - J_E) = 0$ and by substituting the values of M and the fractional orders, $\det(diag[\lambda^{97}, \lambda^{98}, \lambda^{99}] - J_E) = 0$ and the characteristic equation at equilibrium point $E_{1,2}$ is,

$\lambda^{294} + \lambda^{198} + \lambda^{197} \pm 4.5\lambda^{196} \mp 0.004\lambda^{195} + \lambda^{101} \pm 4.5\lambda^{100} + 7.99\lambda^{99} \pm 3.49\lambda^{98} + 5.1\lambda^{97} + \lambda^3 \pm 3.49\lambda^2 + 12.1\lambda \mp 2.61.$

For the values of parameters mentioned in Section 2 the approximated solution of the characteristic equation is $\lambda_{294} = 0.921$ and whose argument is zero and which is the minimum argument and hence the stability necessary condition becomes, $\frac{\pi}{200} - 0 > 0$ which solves for $0.0157 > 0$ and hence the fractional order chaotic chameleon system is stable and chaos exists in the incommensurate system.

6. Conclusions

In this paper, a novel 3D continuous chaotic chameleon is examined with phase portraits. The system has two important properties as self-excited (SA) and hidden attractors (HA). Firstly, we introduced the system which can change between SA and HA depending on the value of parameter. The dynamic properties of the system is presented by numerical simulation in detail. The KY dimension of SA and HA are very good as seen as Table 2. Also, in this paper, real-time engineering applications of system are done as electronic circuit implementation and FPGA-based chaotic oscillator. In addition to, with the introduced chameleon chaotic system is derived its fractional-order form and is made basic dynamic analyses such as bifurcation and stability. Actually, the studying of fractional and non-fractional systems with SA and HA are of recent interest. More different and interesting issues corresponding to these topics will be addressed in other works.

Acknowledgment

This work was partially supported by Sakarya University Scientific Research Projects Unit under Grants 2016-09-00-008, 2016-50-01-026.

References

[1] Leonov GA, Kuznetsov NV, Vagaitsev VI. Localization of hidden chuas attractors. Phys Lett A 2011;375(23):2230–3.
[2] Leonov GA, Kuznetsov NV, Vagaitsev VI. Hidden attractor in smooth chua systems. Physica D 2012;241(18):1482–6.
[3] Leonov GA, Kuznetsov NV. Hidden attractors in dynamical systems. from hidden oscillations in Hilbert–Kolmogorov, Aizerman, and Kalman problems to hidden chaotic attractor in chua circuits. Int J Bifurcation Chaos 2013;23(01):1330002.
[4] Leonov GA, Kuznetsov NV, Mokaev TN. Hidden attractor and homoclinic orbit in lorenz-like system describing convective fluid motion in rotating cavity. Commun Nonlinear Sci Numer Simul 2015;28(1):166–74.
[5] Leonov GA, Kuznetsov NV, Mokaev TN. Homoclinic orbits, and self-excited and hidden attractors in a lorenz-like system describing convective fluid motion. Eur Phys J Spec Top 2015;224(8):1421–58.
[6] Sharma PR, Shrimali MD, Prasad A, Kuznetsov NV, Leonov G. Control of multistability in hidden attractors. Eur Phys J Spec Top 2015;224(8):1485–91.
[7] Sharma PR, Shrimali MD, Prasad A, Kuznetsov NV, Leonov GA. Controlling dynamics of hidden attractors. Int J Bifurcation Chaos 2015;25(04):1550061.
[8] Jafari S, Sprott JC, Pham V-T, Golpayegani SMRH, Jafari AH. A new cost function for parameter estimation of chaotic systems using return maps as fingerprints. Int J Bifurcation Chaos 2014;24(10):1450134.
[9] Pham V-T, Volos C, Jafari S, Wei Z, Wang X. Constructing a novel no-equilibrium chaotic system. Int J Bifurcation Chaos 2014;24(05):1450073.
[10] Tahir FR, Jafari S, Pham V-T, Volos C, Wang X. A novel no-equilibrium chaotic system with multiwing butterfly attractors. Int J Bifurcation Chaos 2015;25(04):1550056.
[11] Jafari S, Pham V-T, Kapitaniak T. Multiscroll chaotic sea obtained from a simple 3d system without equilibrium. Int J Bifurcation Chaos 2016;26(02):1650031.
[12] Lao S-K, Shekofteh Y, Jafari S, Sprott JC. Cost function based on gaussian mixture model for parameter estimation of a chaotic circuit with a hidden attractor. Int J Bifurcation Chaos 2014;24(01):1450010.
[13] Pham V-T, Vaidyanathan S, Volos C, Jafari S, Kingni ST. A no-equilibrium hyperchaotic system with a cubic nonlinear term. Optik-Int J Light Electron Opt 2016;127(6):3259–65.
[14] Pham V-T, Vaidyanathan S, Volos CK, Jafari S, Kuznetsov NV, Hoang TM. A novel memristive time–delay chaotic system without equilibrium points. Eur Phys J Spec Top 2016;225(1):127–36.
[15] Akgul A, Pehlivan I. A new three-dimensional chaotic system without equilibrium points, its dynamical analyses and electronic circuit application, 23. Tech Gaz(Croatia). p. 209–14. (1)
[16] Molaie M, Jafari S, Sprott JC, Golpayegani SMRH. Simple chaotic flows with one stable equilibrium. Int J Bifurcation Chaos 2013;23(11):1350188.
[17] Kingni ST, Jafari S, Simo H, Woafo P. Three-dimensional chaotic autonomous system with only one stable equilibrium: analysis, circuit design, parameter estimation, control, synchronization and its fractional-order form. Eur Phys J Plus 2014;129(5):1–16.
[18] Pham V-T, Jafari S, Volos C, Giakoumis A, Vaidyanathan S, Kapitaniak T. A chaotic system with equilibria located on the rounded square loop and its circuit implementation. IEEE Trans Circuits Syst II 2016;63(9):878–82.
[19] Rajagopal K, Karthikeyan A, Srinivasan AK. FPGA implementation of novel fractional-order chaotic systems with two equilibriums and no equilibrium and its adaptive sliding mode synchronization. Nonlinear Dyn 2017:1–24.
[20] Rajagopal K, Guessas L, Karthikeyan A, Srinivasan AK, Adam G. Fractional order memristor no equilibrium chaotic system with its adaptive sliding mode synchronization and genetically optimized fractional order PID synchronization. Complexity 2017;2017:19. doi:10.1155/2017/1892618. article id 1892618.
[21] Borah M, Roy BK. Hidden attractor dynamics of a novel non-equilibrium fractional-order chaotic system and its synchronisation control. In: Control conference (ICC), 2017 Indian. IEEE; 2017. p. 450–5.
[22] Leon OC. A universal circuit for studying and generating chaos.I. routes to chaos. IEEE Trans CircSyst 1993;40:732–44.
[23] Nakagawa S, Saito T. An RC OTA hysteresis chaos generator. In: Circuits and systems, 1996. ISCAS'96., connecting the world., 1996 IEEE international symposium on, 3. IEEE; 1996. p. 245–8.
[24] Tamasevicius A, Namajunas A, Cenys A. Simple 4d chaotic oscillator. Electron Lett 1996;32(11):957–8.
[25] Ogorzalek MJ. Order and chaos in a third-order RC ladder network with nonlinear feedback. IEEE TransCircSyst 1989;36(9):1221–30.
[26] Kawakami H. Bifurcation of periodic responses in forced dynamic nonlinear circuits: computation of bifurcation values of the system parameters. IEEE TransCircSyst 1984;31(3):248–60.
[27] SAITO T. Chaotic phenomena in a coupled oscillators. In: Circuit theory and design 87: proceedings of the European conference on circuit theory and design–ECCTD 87, Paris, France, 1–4 September 1987. North Holland; 1987. p. 275.
[28] Chua LO, Lin T. Chaos and fractals from third-order digital filters. Int J Circuit Theory Appl 1990;18(3):241–55.
[29] Chua LO, Lin T. Fractal pattern of second-order non-linear digital filters: a new symbolic analysis. Int J Circuit Theory Appl 1990;18(6):541–50.
[30] Hamill DC, Jeffries DJ. Subharmonics and chaos in a controlled switched-mode power converter. IEEE Trans Circ Syst 1988;35(8):1059–61.
[31] Poddar G, Chakrabarty K, Banerjee S. Control of chaos in the boost converter. Electron Lett 1995;31(11):841–2.
[32] Li C, Pehlivan I, Sprott JC, Akgul A. A novel four-wing strange attractor born in bistability. IEICE Electron Express 2015;12(4):20141116.
[33] Akgul A, Moroz I, Pehlivan I, Vaidyanathan S. A new four-scroll chaotic attractor and its engineering applications. Optik-Int J Light Electron Opt 2016;127(13):5491–9.
[34] Akgul A, Hussain S, Pehlivan I. A new three-dimensional chaotic system, its dynamical analysis and electronic circuit applications. Optik-Int J Light Electron Opt 2016;127(18):7062–71.
[35] Akgul A, Pehlivan I. A new three-dimensional chaotic system without equilibrium points, its dynamical analyses and electronic circuit application, 23. Tech Gaz(Croatia). p. 209–14. (1)
[36] Kaçar S. Analog circuit and microcontroller based rng application of a new easy realizable 4d chaotic system. Optik-Int J Light Electron Opt 2016;127(20):9551–61.
[37] Akgul A, Li C, Pehlivan I. Amplitude control analysis of a four-wing chaotic attractor, its electronic circuit designs and microcontroller-based random number generator. J Circ, Syst Comput 2017:1750190.
[38] Kai G, Zhang W, Wei ZC, Wang JF, Akgul A. Hopf bifurcation, positively invariant set, and physical realization of a new four-dimensional hyperchaotic financial system. Math Prob Eng 2017;2017.
[39] Wei Z, Moroz I, Sprott JC, Akgul A, Zhang W. Hidden hyperchaos and electronic circuit application in a 5d self-exciting homopolar disc dynamo. Chaos 2017;27(3):033101.
[40] Pham V-T, Akgul A, Volos C, Jafari S, Kapitaniak T. Dynamics and circuit realization of a no–equilibrium chaotic system with a boostable variable. AEU-Int J ElectronCommun 2017.
[41] Wang Z, Akgul A, Pham V-T, Jafari S. Chaos-based application of a novel no-equilibrium chaotic system with coexisting attractors. Nonlinear Dyn 2017:1–11.
[42] Kuon I, Tessier R, Rose J. Fpga architecture: survey and challenges, 2. Foundations and Trends in Electronic Design Automation; 2008. p. 135–253. (2)

[43] Munden R. ASIC and FPGA verification: a guide to component modeling. Academic Press; 2004.
[44] Tuna M, Fidan CB. Electronic circuit design, implementation and FPGA-based realization of a new 3d chaotic system with single equilibrium point. Optik-Int J Light Electron Opt 2016;127(24):11786–99.
[45] Nguyen AH, Pickering MR, Lambert A. The FPGA implementation of a one-bit-per-pixel image registration algorithm. J Real-Time Image Process 2016;11(4):799–815.
[46] Avaroglu E, Tuncer T, Özer AB, Türk M. A new method for hybrid pseudo random number generator. Informacije MIDEM 2015;44(4):303–11.
[47] Koyuncu İ, Özcerit AT. The design and realization of a new high speed FPGA-based chaotic true random number generator. Comput Electr Eng 2016.
[48] Volos C, Akgul A, Pham V-T, Stouboulos I, Kyprianidis I. A simple chaotic circuit with a hyperbolic sine function and its use in a sound encryption scheme. Nonlinear Dyn 2017:1–15.
[49] Bittner R, Ruf E, Forin A. Direct GPU/FPGA communication via PCI express. Cluster Comput 2014;17(2):339–48.
[50] Maldonado Y, Castillo O, Melin P. A multi-objective optimization of type-2 fuzzy control speed in FPGAs. Appl Soft Comput 2014;24:1164–74.
[51] Koyuncu İ, Şahin İ, Gloster C, Sarıtekin NK. A neuron library for rapid realization of artificial neural networks on FPGA: a case study of rössler chaotic system. J Circ, Syst Comput 2017;26(01):1750015.
[52] Çavuşlu MA, Karakuzu C, Şahin S, Yakut M. Neural network training based on FPGA with floating point number format and its performance. In: Neural computing and applications, 20; 2011. p. 195–202. (2)
[53] Danca M-F. Hidden chaotic attractors in fractional-order systems. Nonlinear Dyn 2017:1–10.
[54] Li RH, Chen WS. Fractional order systems without equilibria. Chin Phys B 2013;22:040503.
[55] Cafagna D, Grassi G. Fractional-order systems without equilibria: the first example of hyperchaos and its application to synchronization. Chin Phys B 2015;24(8):080502.
[56] Baleanu D, Diethelm K, Scalas E, Trujillo JJ. Fractional calculus: models and numerical methods, 5. World Scientific; 2016.
[57] Zhou Y, Wang JR, Zhang LU. Basic theory of fractional differential equations. World Scientific; 2016.
[58] Diethelm K. The analysis of fractional differential equations: an application-oriented exposition using differential operators of Caputo type. Springer; 2010.
[59] Kaçar S, Akgül A, Ergüzel AT, Öztürk MM, Sevin A. Design of a web interface for fractional chaotic systems. Int J Comput NetwInf Secur (IJCNIS) 2014;7(1):46.
[60] Aghababa MP. Robust finite-time stabilization of fractional-order chaotic systems based on fractional lyapunov stability theory. J Comput Nonlinear Dyn 2012;7(2):021010.
[61] Boroujeni EA, Momeni HR. Non-fragile nonlinear fractional order observer design for a class of nonlinear fractional order systems. Signal Process 2012;92(10):2365–70.
[62] Zhang R, Gong J. Synchronization of the fractional-order chaotic system via adaptive observer. Syst Sci Control Eng 2014;2(1):751–4.
[63] Danca M-F, Tang WKS, Chen G. Suppressing chaos in a simplest autonomous memristor-based circuit of fractional order by periodic impulses. Chaos, Solitons Fractals 2016;84:31–40.
[64] Petráš I. Method for simulation of the fractional order chaotic systems. Acta Montanistica Slovaca 2006;11(4):273–7.
[65] Trzaska Z. Matlab solutions of chaotic fractional order circuits. chapter 19 in: all assi. Engineering education and research using MATLAB. Intech, Rijeka; 2011.
[66] Petras I. Fractional-order nonlinear systems: modeling, analysis and simulation. Springer Science & Business Media; 2011.
[67] Jafari MA, Mliki E, Akgul A, Pham V-T, Kingni ST, Wang X, et al. Chameleon: the most hidden chaotic flow. Nonlinear Dyn 2017:1–15.
[68] Rajagopal K, Karthikeyan A, Duraisamy P. Hyperchaotic chameleon: fractional order FPGAimplementation. Complexity 2017. https://www.hindawi.com/journals/complexity/aip/8979408/.
[69] Li C, Gong Z, Qian D, Chen YQ. On the bound of the lyapunov exponents for the fractional differential systems. Chaos 2010;20(1):013127.
[70] Wolf A, Swift JB, Swinney HL, Vastano JA. Determining Lyapunov exponents from a time series. Physica D 1985;16(3):285–317.
[71] Ellner S, Gallant AR, McCaffrey D, Nychka D. Convergence rates and data requirements for Jacobian-based estimates of Lyapunov exponents from data. Phys Lett A 1991;153(6–7):357–63.
[72] Maus A, Sprott JC. Evaluating lyapunov exponent spectra with neural networks. Chaos, Solitons Fractals 2013;51:13–21.
[73] Tavazoei MS, Haeri M. Unreliability of frequency-domain approximation in recognising chaos in fractional-order systems. IET Signal Proc 2007;1(4):171–81.